EVOLUTION OF REE, Sr AND Ba ABUNDANCES DURING LUNAR IGNEOUS DIFFERENTIATION, D. Weill, G. McKay, S. Kridelbaugh, and M. Grutzeck, Center for Volcanology, University of Oregon, Eugene, Or., 97403.

Experimental measurements (1,2,3) of sol/liq distribution coefficients for plagioclase (PL) and clinopyroxene (CPX) permit systematic analysis of the evolution of abundance patterns. The contrasting effect of crystallizing PL and CPX can be seen in fig. 1, summarizing experiments at 1250°C in the "near-basalt" system Ab-An-Di. Effect of f_{O_2} on D_{Eu} is explained in fig. 2. The curve shows variation of D_{Eu} between D_3 limiting values of D_3 and D_2 calculated on the basis of an oxidation state distribution proportional to $f_{O_2}^{1/4}$ (2). Experimental points are also shown. T variation is approximated by Arrhenius equations. A summary of the experimental data is shown in fig. 3. Differences between D_3 and $D_{Sr} \wedge D_2$ are a measure of the maximum attainable Eu-anomaly, and the data unequivocally demonstrate a negative anomaly potential in CPX down to at least 1100°. The T-dependence of D_{Eu} is drawn assuming a lunar T-f_{O_2} trend of .03xIW (4).

Crystallization at low P is approximated by the pseudoternary in fig. 4 (5). Two contrasting crystallization sequences are shown along with a proposed highland avg. comp. (6). Early igneous differentiation may have produced PL-rich high level crust with mafic complements at lower levels. The original comp. must be concentrated in mafic components relative to present highlands (HL). Points 1 and 2 are possibilities chosen to calculate the evolution of trace element abundances during fractional crystallization with variable D's. A typical result is shown in fig. 5. The relative abundances developed in L, PL and CPX between .40 and .02 L remaining is shown in fig. 6. Absolute and relative enrichments in the liquid at L < .10 are grossly comparable to KREEP if the original liquid is assumed 10-15x chondrites. Sequence 2-3-R develops small positive anomalies in early stage L and less extreme late stage negative anomalies than sequence 1-R which is dominated by PL crystallization. Systematic differences also occur in the mineral phase patterns, but in the later stages of fractionation all patterns are similar to those found in lunar minerals and rocks. Based only on considerations of the general appearance of the abundance patterns of these elements, it is difficult to rule out the possibility that fractionated liquids of this type formed veins, dikes or sills in the early crust and are now contributing to the general KREEP level. The fine structure of the correlation between the Eu-anomaly (Sm/Eu) and the absolute enrichment in REE (Sm) shows that sequence 1-R results in Sm/Eu larger relative to Sm than found in KREEP (fig. 7). Fractionation sequence 2-3-R is more compatible with KREEP. Although PL is necessary for the Eu-anomaly signature of KREEP, sequence 1-R provides too much of a good thing. Enrichment of high crustal levels in PL probably resulted from gravity separation of mafics. In fig. 8 we show the effect of removing sufficient OL and PX to change the bulk compositions of 1 and 2 to HL. The resulting patterns are compared to the HL REE abundances (6). Removing OL + CPX from 2 yields a pattern with slight relative enrichment in light REE similar to HL but also a small positive anomaly not suggested for HL. If half of PX removed is OPX (OL and OPX are assigned D < .01), the anomaly

EVOLUTION OF REE ABUNDANCES
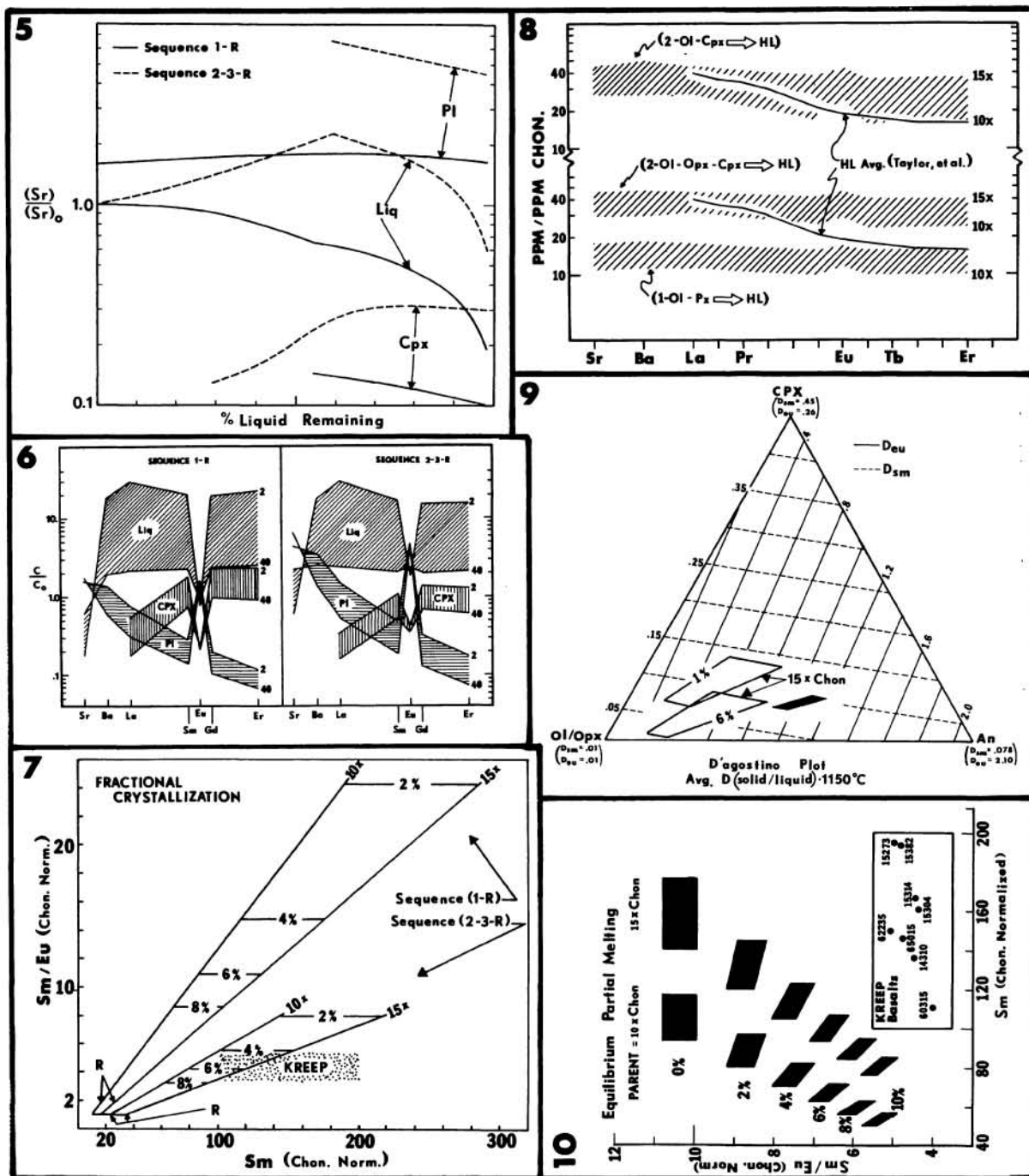
Weill, D., et al.

is reduced, but the enrichment in heavy REE is high. Composition 1 (already close to HL) is not significantly affected by the process.

Partial melting may be a preferred mechanism for generating KREEP. Analysis of partial melting can best be visualized with D'agostino diagrams. In figs. 9-10 we illustrate the systematics of the Sm vs Sm/Eu trends in partial melting. The PL-CPX-(OL+OPX) triangle is contoured in D_{Sm} and D_{Eu}. For a given degree of equilibrium melting, each composition uniquely determines a set of Sm and Sm/Eu values. The blacked area in fig. 9 gives rise to a corresponding area in fig. 10 at each melting interval, and the family of areas delineates the trend of partial melting. Conversely, the KREEP rectangle in fig. 10 has counterpart areas in fig. 9 (shown at 1 & 6% melting) which outline the phase composition limits capable of generating melts within the KREEP rectangle. The parameters used in fig. 9 place strict limitations on the amounts of PL and CPX in the source rock.
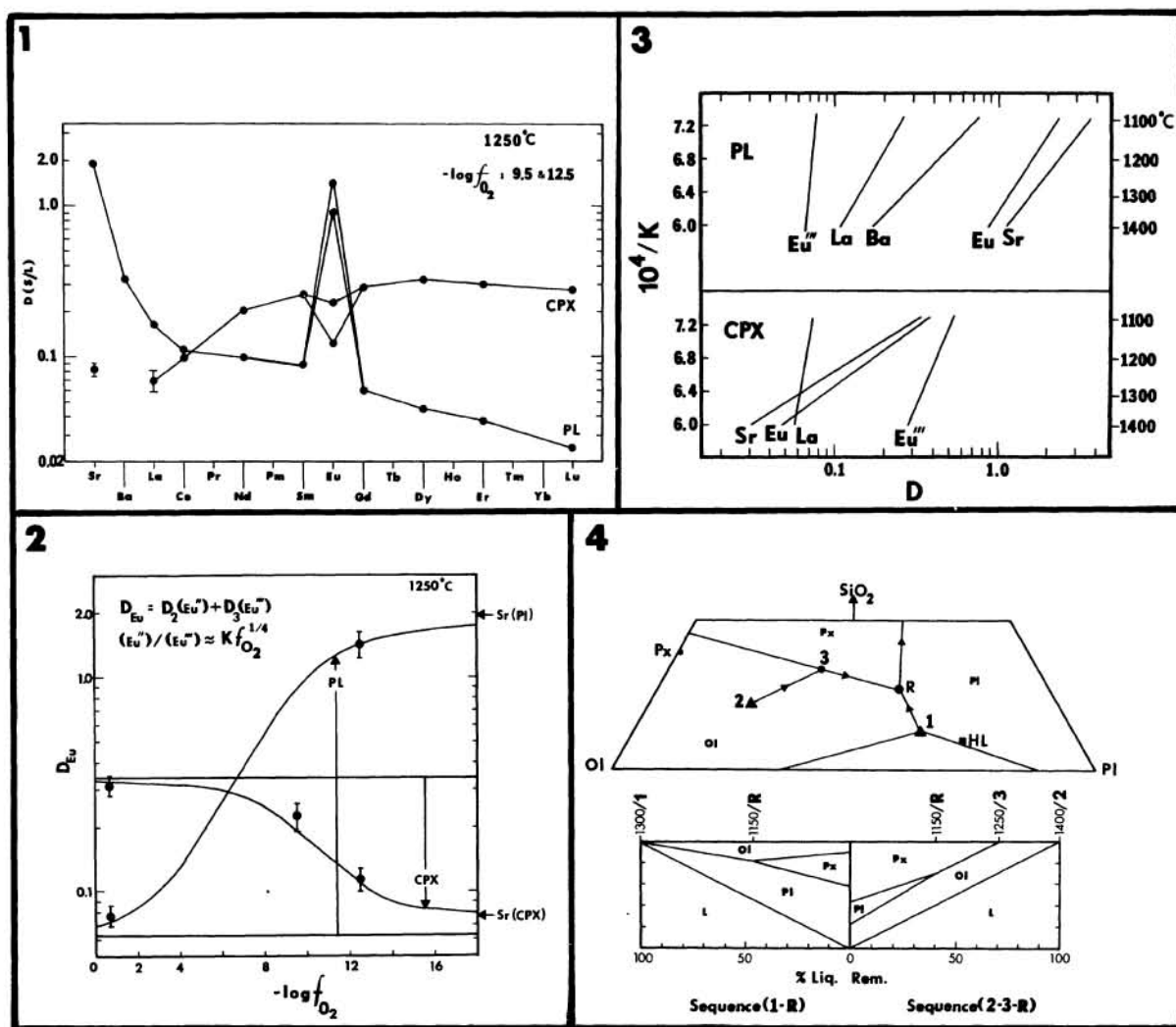
EVOLUTION OF REE ABUNDANCES

Weill, D., et al.

REFERENCES: (1) Drake, M.(1972) Ph.D. Thesis, U. Oregon (2) Weill, D. and M. Drake (1973) Science, 180, 1059 (3) Grutzeck et al.(1973) Trans. AGU, 54, 1222 (4) Sato, M. et al. (1973) GCA Suppl 4, 1, 1061 (5) Walker, D. et al. (1972) GCA Suppl 3, 1, 797 (6) Taylor, S. et al. (1973) GCA Suppl 4, 2, 1445.